The LHCb Silicon Tracker – Performance & Radiation Damage

Proceedings of the 9th International Conference on Radiation Effects on Semiconductor Materials Detectors and Devices (RESMDD12)

The LHCb Silicon Tracker group

Ch. Elsasser[c,1], B. Adeva[a], A. Gallas[a], E. Pérez Trigo[a], P. Rodríguez Pérez[a], Y. Amhis[b,f], A. Bay[b], F. Blanc[b], G. Cowan[b,g], F. Dupertuis[b], V. Fave[b], G. Haefeli[b], I. Komarov[b], J. Luisier[b], R. Märki[b], B. Muster[b], T. Nakada[b], O. Schneider[b], M. Tobin[b], M.T. Tran[b], J. Anderson[c], A. Bursche[c], N. Chiapolini[c], M. De Cian[c,h], C. Salzmann[c], S. Saornil[c], S. Steiner[c], O. Steinkamp[c], U. Straumann[c], A. Vollhardt[c], O. Aquines Gutierrez[d], M. Britsch[d], M. Schmelling[d], H. Voss[d], V. Iakovenko[e], O. Okhrimenko[e], V. Pugatch[e]

(a) University of Santiago de Compostela, Santiago de Compostela, Spain.
(b) Ecole Polytechnique Fédérale de Lausanne (EPFL), Lausanne, Switzerland.
(c) Physik-Institut, Universität Zürich, Zürich, Switzerland.
(d) Max Planck Institut für Kernphysik (MPIK), Heidelberg, Germany.
(e) National Academy of Sciences, Institute for Nuclear Research, Kiev, Ukraine.
(f) Now at LAL, Université Paris-Sud, CNRS/IN2P3, Orsay, France.
(g) Now at School of Physics and Astronomy, University of Edinburgh, Edinburgh, United Kingdom.
(h) Now at Physikalisches Institut, Ruprecht-Karls-Universität Heidelberg, Heidelberg, Germany.

Abstract

The LHCb experiment is searching for New Physics and performing high-precision measurements of CP violation with the high rate of beauty and

[1]Corresponing author:
Physics Institute, University Zurich
Winterthurerstrasse 190
CH-8057 Zurich
che@physik.uzh.ch

charmed hadrons produced in the pp collisions at LHC. The LHCb detector is set-up as a single-armed forward spectrometer with excellent tracking and particle identification capabilities. A part of the tracking system measuring the particle trajectories to a very high precision is formed by the Silicon Tracker. This paper reports on the performance of the Silicon Tracker during the data taking at LHC. Furthermore, it shows radiation damage studies based on leakage currents and also on charge collection efficiency scans for the first time.

Keywords:
LHCb, Silicon Tracker, Radiation Damage, Alignment

---

1. The LHCb Silicon Tracker

The LHCb Silicon Tracker is a part of the tracking system of the LHCb detector [1] and consists of about 12 m^2 of sensitive area with approximately 272k read-out channels. The tracker is divided into two sub-detectors, the Tracker Turicensis (TT) placed upstream from the dipole magnet; and the Inner Tracker (IT) forming the inner part of the tracking stations downstream from the dipole magnet.
Both sub-detectors are made of silicon micro-strip sensors. In case of TT there are four detector layers (0°, +5°, −5° and 0° tilted). The sensors are p-on-n type, have a pitch of 183 µm and a thickness of 500 µm. The sensors are grouped to read-out sectors consisting of either 1, 2, 3 or 4 sensors. This leads to read-out strips of up to 37 cm in length.
The IT is also made of p-on-n sensors with a pitch of 198 µm. The sensors are paired to form a read-out sector having a strip length of 22 cm. In this case, the sensors used are 410 µm thick and this configuration is used on both sides of the beam pipe. Below and above the beam pipe the read-out sectors consist of only one sensor with a thickness of 320 µm and a read-out strip length of 11 cm. The Inner Tracker consists of a total of twelve detection layers grouped into three stations with four layers.
Both detectors are operated at a temperature of 0° C leading to a sensor temperature of about 8° C.

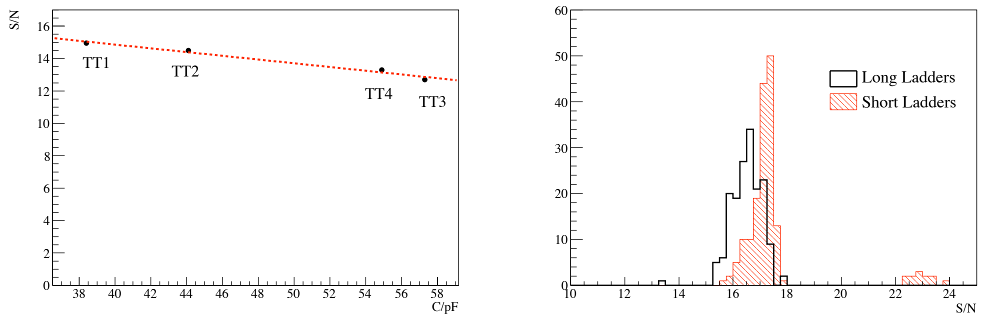

Figure 1: Left: Signal-to-Noise ratio versus measured capacitance for the four types of read-out sectors in TT. The number indicates the number of sensors in the particular sector type. The three-sensor type (TT3) has a higher capacitance than the four-sensor one (TT4) due to the additional Kapton cable connecting it to the read-out electronics; Right: Distribution of Signal-To-Noise ratio for long and short ladders in IT. The peak at high values is due to the usage of thick sensors in short ladders.

2. Performance

2.1. General Performance

At the time of the conference (October 2012) the tracker had 99.7 % of the channels working in TT and 98.7 % in IT. The lower percentage in case of IT is caused by two non-configurable read-out sectors as well as several dead VCSEL[2] diodes. These diodes are used to transmit the data from the read-out electronics on the detector to the counting house and cannot be easily replaced as it is difficult to access the electronics without opening the detector. These problems will be cleared during the Long Shotdown 1.

2.2. Signal-to-Noise Ratio

The Signal-to-Noise Ratio (S/N) is measured by using clusters which are assigned to tracks with a momentum $p > 5\,\mathrm{GeV/c}$. The ratio is between 12 and 15 for TT, and is shown in Fig. 1 for the different strip capacitances. The three-sensor configuration has a higher capacitance and a lower S/N than those with four sensors, as the three-sensor sectors are connected to the electronics via a Kapton cable while the four-sensor sectors are connected

[2]VCSEL: vertical-cavity surface-emitting laser

directly. In case of IT we measure for the short and long ladders a S/N of 17.5 and 16.5 respectively (cf. Fig. 1). The peak around S/N of 23 is due to 410 μm thick sensors used in short ladders instead of the usual 320 μm ones. All values obtained are within 10 to 20 % of those expected from prototype measurements [2].

2.3. Spatial Alignment

The spatial alignment of the detector is based on a global χ^2 minimisation using Kalman track residuals. Further information from a sample of decay vertices from $D^0 \rightarrow K^-\pi^+$ and $J/\psi \rightarrow \mu^+\mu^-$ with constrained invariant mass is taken as an additional requirement [3, 4].

Fig. 2 shows the distribution of unbiased and biased residuals. The unbiased residuals are taken for all clusters as the distance between the extrapolated track position after removing the hit from the track fit and the hit. The biased residuals are the distribution of mean of unbiased residuals in each sector.

The alignment precision is calculated as the RMS of the biased residual distribution and is about 14 μm for both sub-detectors . Considering the fact that in LHCb there are long distances between the tracking stations and additional sub-detectors inbetween as well as that the stations are not inside the magnetic field, this value is extremely good.

The hit resolution is taken as the RMS after removing the biased residual component from the unbiased residuals. It is 59 μm and 50 μm for TT and IT respectively.

2.4. Hit Efficiency

The hit efficiency is measured from data using tracks from $D^0 \rightarrow K^+K^-$ with momentum $p > 10\,\mathrm{GeV/c}$. The tracks are extrapolated to the sensors and hits are searched in a window around the extrapolated track position. In both sub-detectors an average hit efficiency of over 99 % is achieved.

3. Radiation Damage

The radiation damage in the Silicon Tracker is measured in two different ways: The first method uses the leakage current while the second one uses data which is taken during a charge collection efficiency scan where different bias voltages are applied.

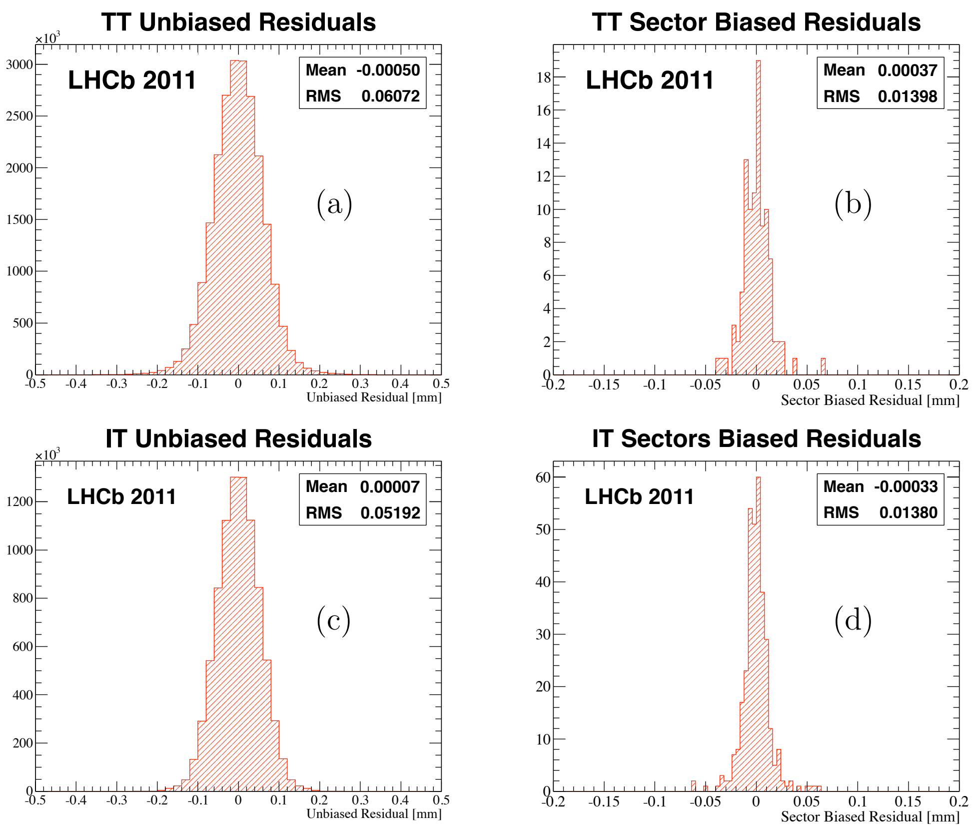

Figure 2: Distribution of unbiased cluster residuals in TT (a) and IT (c). Biased sector residuals in TT (b) and IT (d). All quantities are indicated in millimeters. Details about the calculation are described in the text.

3.1. Leakage Current

In silicon sensors, bulk damage caused by the radiation leads to an increased leakage current ΔI_{leak} which is directly related to the fluence by

$$\Delta I_{\text{leak}} = \alpha \cdot \Phi_{eq} \cdot V, \tag{1}$$

where Φ_{eq} is the 1-MeV neutron equivalent fluence, V the volume of the irradiated silicon and α the temperature dependent damage factor for 1-MeV neutrons [5].
Fig. 3 shows the delivered luminosity and the peak current for the different HV sectors for TT and IT. In both cases we see a good agreement between the luminosity and the peak current.
The peak current shows, as expected, a decrease during periods without colliding beams (shutdowns and technical stops) due to annealing in the silicon.

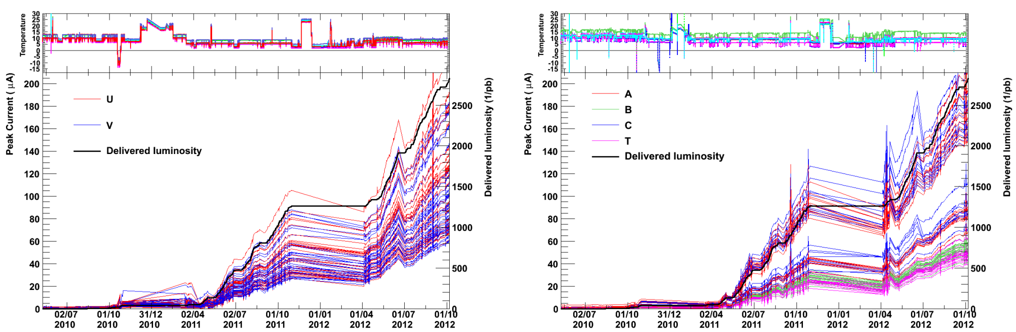

Figure 3: Measured peak currents per fill and HV sector shown as a function of time for TT (left) and IT (right). The delivered integrated luminosity for LHCb is shown in black. A good agreement between the progress of the two quantities is seen. During periods of shutdowns or technical stops annealing takes place leading to a decrease of the peak currents. Above the plot of the current, the temperature values within the detector boxes are shown as a function of time.

3.2. Charge Collection Efficiency Scans

The goal of the charge collection efficiency (CCE) scans is to measure the full-depletion voltage V_d of the sensors. In these scans, the bias voltage, V_{bias}, and the sampling time are varied. The variation of the later takes differences in the charge collection time due to different V_{bias} into account. The changes are only made in one layer in both TT and IT. Therefore, the other layers can be still used to reconstruct tracks. These tracks are then extrapolated to the scanned layers. The sum of the ADC values of the three strips closest to the extrapolated track position are taken as the ADC value associated to this track.

Fig. 4 shows the ADC value distribution in a readout sector for a certain timing and voltage configuration. The noise distribution around zero represents tracks created by associating hits from different particles to a so-called ghost track as well as extrapolations where the predicted track point is too far away from the actual hit.

By fitting the distribution with a Landau function convolved with a double Gaussian we can extract the most probable value from the signal distribution. From the different sampling times for a certain voltage step we can extract the pulse shape shown in Fig. 5. This is fitted with a Half-Gaussian to extract the maximum ADC value.

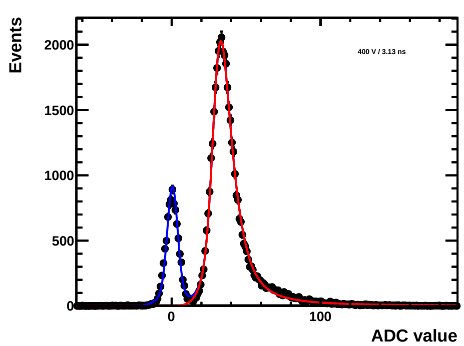

Figure 4: The distribution of the summed ADC values of the three strips around the extrapolated track position at the scanned layer. The fitted signal distribution (Landau distribution convoluted with double Gaussian) is shown in red while the noise distribution is fitted by a double Gaussian (blue).

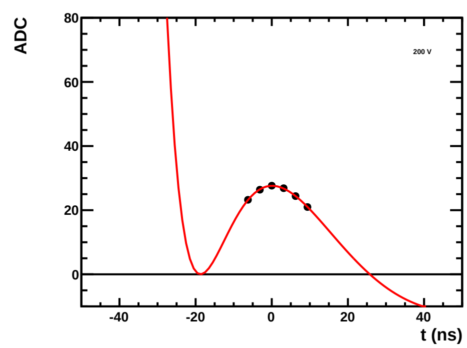

Figure 5: Pulse shape taken from the different sample timing steps and fitted with a Half-Gaussian function.

Fig. 6 shows the maximum ADC values as a function of V_{bias}. The data points are fitted with a sigmoid function

$$ADC_{\max}(V_{\text{bias}}) = \frac{A_0}{1 + \exp r(V_{\text{bias}} - V_0)}, \tag{2}$$

and the full-depletion voltage is extracted as the value of the bias voltage when the function reaches 80 % of its maximum value. The value of 80 % has been chosen by comparing the earliest CCE scan and the V_d measured during the production of the detector modules.

In Fig. 7 the measured V_d values as a function of time are shown for the TT read-out sector closest to the beam pipe where only tracks passing the sensor within 45 mm of the beam axis are considered. The depletion voltage has decreased by about 70 V since the beginning of data taking.
The expectation from the Hamburg model [6] applied to the LHCb running conditions (average instantaneous luminosity per fill, fluence profile simulated by FLUKA and measured temperature in the detector box) is shown in black. The initial value of V_d is taken as the one measured after production. The parameters for the Hamburg model used in the simulation are listed in Tab. 1. A good agreement between the measured V_d values and the predicted progress of V_d is seen.

4. Conclusion

The LHCb Silicon Tracker is a part of the LHCb tracking system consisting of two sub-detectors: The Tracker Turicensis and the Inner Tracker.
Both sub-detectors work extremely well with more than 99.7 % (TT) and 98.7 % (IT) of the channels working. The measured Signal-to-Noise ratios are in the range 12-15 (TT) and 16-18 (IT) which is close to the expectations from test beam measurement.
The hit efficiency of the Silicon Tracker is above 99 % for both sub-detectors. The TT has a hit resolution of 59 μm while the IT achieves one of 50 μm. Both sub-detectors could be aligned with a precision of better than 14 μm. The radiation damage is monitored by measuring the leakage currents and the full-depletion voltage measured in charge collection efficiency scans. Both methods show a good agreement between the measured values and the expectation based on the running conditions of LHCb. The measured effects of the radiation damage so far show no sign of type-inversion even in the most irradiated part of the Silicon Tracker. Type inversion in the highly

Table 1: Parameters used in the Hamburg model to create predictions for V_d [6].

Parameter	Value
g_a	$1.4 \cdot 10^2\,\mathrm{cm}^{-1}$
$k_{0,a}$	$2.4 \cdot 10^{13}\,\mathrm{s}^{-1}$
E_{aa}	$1.086\,\mathrm{eV}$
g_Y	$5.7 \cdot 10^2\,\mathrm{cm}^{-1}$
$k_{0,Y}$	$1.5 \cdot 10^{15}\,\mathrm{s}^{-1}$
E_Y	$1.3125\,\mathrm{eV}$
g_c	$1.6 \cdot 10^2\,\mathrm{cm}^{-1}$
$N_{C0} \cdot c$	$7.5 \cdot 10^{-2}\,\mathrm{cm}^{-1}$

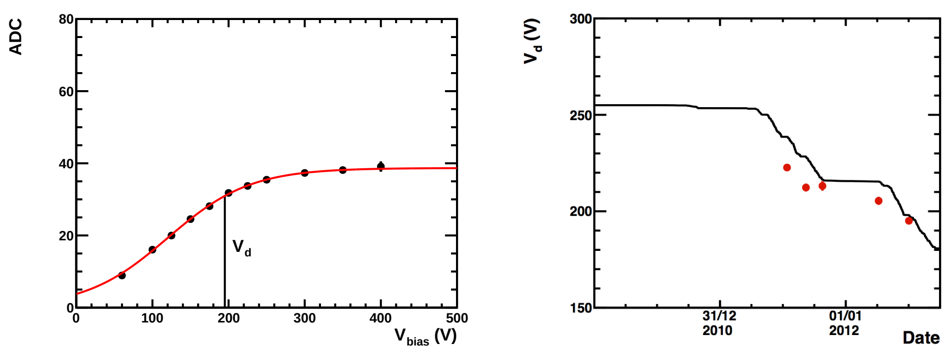

Figure 6: Maximal ADC values as a function of the bias voltage V_{bias} for the area within 45 mm to the beam axis of the readout sector closest to the beam pipe. The black points are the data taken from different voltage steps while the red line is a sigmoid function fitted to the data. The full-depletion voltage is defined as the voltage where the function reaches 80 % of its maximum value.

Figure 7: Full-depletion voltage V_d as a function of time. The red dots represent the values determined from the CCE scans and the black line shows the expected progress derived from the Hamburg model.

irradiated areas is expected to be seen during the next LHC runs before a possible upgrade of LHCb.

[1] A. A. Alves *et al.*, *JINST* **3** (2008), S08005.

[2] M. Agari *et al.*, Test beam results of multi-geometry prototype sensors for the LHCb Inner Tracker, LHCb-2002-058.

[3] W. Hulsbergen, *Nucl. Inst. Meth.* **A600**, 471 (2009).

[4] J. Amoraal *et al.*, Application of vertex and mass constraints in track-based alignment, arXiv:1207.4756v1

[5] M. Moll *et al.*, *Nucl. Inst. Meth.* **A426**, p. 87 (1999).

[6] M. Moll, Radiation Damage in Silicon Particle Detectors, DESY-THESIS-1999-040.